MedChemComm

Accepted Manuscript

ROYAL SOCIETY OF CHEMISTRY

www.rsc.org/medchemcomm

Cite this: DOI: 10.1039/c0xx00000x

www.rsc.org/xxxxxx

ARTICLE TYPE

Small-Molecule Phosphodiesterase Probes: Discovery of Potent and Selective CNS-Penetrable Quinazoline Inhibitors of PDE1

John M. Humphrey, *[a] Eddie Yang, [a] Christopher W. am Ende, [a] Eric P. Arnold, [a] Jenna L. Head, [a] Stephen Jenkinson, [b] Lorraine A. Lebel, [a] Spiros Liras, [c] Jayvardhan Pandit, [a] Brian Samas, [a] Felix Vajdos, [a] and Frank S. Menniti. [*d]

Received (in XXX, XXX) Xth XXXXXXXXX 20XX, Accepted Xth XXXXXXXXX 20XX
DOI: 10.1039/b000000x

ABSTRACT: PDE1 is a family of calcium-activated, dual substrate phosphodiesterases expressed in both the CNS and periphery that play a role in the integration of intracellular calcium and cyclic nucleotide signaling cascades. Exploration of the potential in targeting this family of enzymes to treat neuropsychiatric disorders has been hampered by a lack of potent, selective, and brain penetrable PDE1 inhibitors. To identify such compounds we used high-throughput screening, structure-based design, and targeted synthetic chemistry to discover the 4-aminoquinazoline **7a** (PF-04471141) and the 4-indanylquinazoline **27** (PF-04822163) each of which are PDE1 inhibitors that readily cross the blood brain barrier. These quinazoline-based PDE1-selective inhibitors represent valuable new tools to study the biological processes regulated by PDE1 and to begin to determine the potential therapeutic utility of such compounds to treat neuropsychiatric disorders.

Introduction

The cyclic nucleotide phosphodiesterases (PDEs) are a group of enzymes that regulate intracellular signaling through metabolic inactivation of the second messengers cyclic guanosine monophosphate (cGMP) and cyclic adenosine monophosphate (cAMP). The PDEs are encoded by 21 genes that are grouped into eleven different families. The division is based on primary sequence homology that gives rise to family specific substrate specificity, composition of the N-terminal regulatory domain, and sensitivity to pharmacological inhibitors.[1,2] PDE isoform activity is itself regulated through differential tissue expression, cell compartmentalization and activation or inhibition by various cell components.[3] Signal transduction cascades mediated by the cyclic nucleotides and regulated by the PDEs are diverse and include neurotransmission, metabolism, smooth muscle contraction, odorant, taste and visual responses, gene activation, insulin response, locomotion, cell proliferation and cell death among others.[4] Thus, pharmacological manipulation of these signaling cascades through PDE inhibition is of considerable therapeutic interest.[4,5]

The present work focuses on PDE1, which has been extensively studied but for which there is still a deficiency of potent and selective pharmacological tools.[4,6] PDE1 was first isolated in 1970 from bovine[7] and rat brain,[8] with the defining characteristic of stimulation of enzyme activity by calcium/calmodulin.[6] PDE1 isoenzymes are encoded by three genes, PDE1A, PDE1B, and PDE1C. The N-terminal regions contain the regulatory calcium/calmodulin binding sites that activate the enzyme to increase V_{max}. Despite high structural homology within the C-terminal catalytic regions, the three PDE1 isoforms differ in substrate affinity which suggests a level of functional differentiation. Whereas each isoform hydrolyzes cGMP with comparable affinity, their affinities for cAMP differ by as much as two orders of magnitude with the rank order PDE1C > PDE1B > PDE1A.[6] Further indication that the isozymes mediate distinct functions is indicated by the differential isoform distribution throughout the body. For example, while each appears to be present throughout the brain, the expression level of PDE1B in the striatum is much higher than that of PDE1A or PDE1C. Conversely, PDE1C is to be particularly highly expressed in the olfactory epithelium, heart and bladder.[9,10]

Given the regulation of enzymatic activity by calcium, PDE1 appears to be an integration point for intracellular calcium and cyclic nucleotide signaling cascades. In addition to differential tissue distribution, PDE1 isoforms assume distinct roles in CNS function. PDE1B knock-out mice have a phenotype consistent with high striatal expression, including increased locomotor activity and increased phosphorylation of striatal PKA substrates

in response to dopamine agonists.[11] This data suggests the possible use of PDE1B inhibitors in the treatment of attention deficit hyperactivity disorder or Parkinson's disease. Other evidence associating PDE1A gene polymorphism to remission with antidepressant treatment suggests a therapeutic utility in the treatment of depression.[12] Recent reports suggest potential for selective PDE1 inhibitors as cognition enhancers[13] and in the treatment of Huntington's Disease.[14]

To further investigate the role of PDE1 in the regulation of brain function and to begin to explore therapeutic utility, we undertook an effort to discover potent, selective, and brain penetrable inhibitors of PDE1 that would enable isolation of biological effects mediated by PDE1 from those linked to other PDE families. Our approach, which included high throughput screening, structure based design, and parallel and directed synthesis, yielded a series of 4-aminoquinazoline and 4-benzylquinazoline PDE1 inhibitors that readily cross the blood brain barrier. The highlighted compounds from this effort, aminoquinazoline **7a** (PF-04471141) and indanylquinazoline **27** (PF-04822163), are among the most potent and selective small molecule inhibitors of PDE1 reported to date.[15]

Results

For the purposes of chemical library screening and SAR development we used recombinant full-length human PDE1B as a representative of the PDE1 family. This effort began with the identification of the two resynthesized quinazoline file screen hits **1** and **2** (PDE1B IC_{50} 219 nM and 130 nM, respectively, Figure 1). These compounds immediately attracted our attention because of their structural resemblance to known PDE10A inhibitors[16] and physical properties predictive of good central exposure.[17,18] In addition, our prior work on PDE10A inhibitors afforded intimate knowledge of the binding mode of the 6, 7-dimethoxyquinazolines through a crystal structure of PDE10A with bound inhibitor **3**.[16] Key interactions included a bidentate hydrogen bonding interaction between a PDE-invariant glutamine residue and the 6,7-dimethoxy groups (Figure 2). Based on the similar structures of PDE10A and PDE1B, and on the presence of a 6,7-dimethoxy array in the screen hits **1** and **2**, we supposed that a similar binding mode was in effect for PDE1.

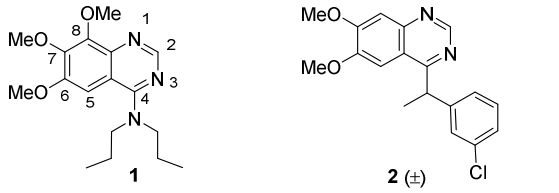

Figure 1. Quinazoline hits **1** and **2** from a high throughput screen.

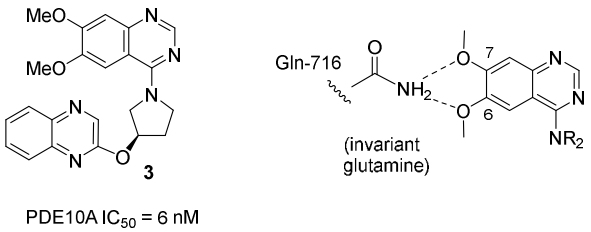

Figure 2. PDE10A inhibitor **3** and key interaction with invariant glutamine residue.

Beginning with the HTS hits, we set about SAR exploration in two ways. We first assessed quinazoline substituent effects utilizing library synthesis to expand the di-*n*-propyl amine series (**1**).[19,20] The templates utilized for these library efforts include the ten 4-chloroquinazoline templates **4a-j** (Figure 3), which were obtained from our in-house sample bank, commercial suppliers, and chemical synthesis. The synthesized 4-chloroquinazolines were generally prepared from anthranilic acid derivatives through the Niementowski quinazoline synthesis according to established methods[21,22] with the exception of **4b** which was prepared via the route shown in Figure 8. The templates were then coupled with a broad set of amines in a parallel format (Figure 3).

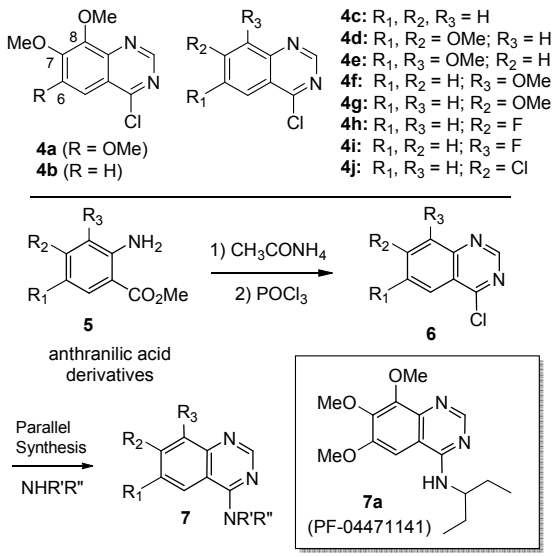

Figure 3. Quinazolines employed in parallel synthesis, and quinazoline synthesis from anthranilic acid.

The amines for the libraries were sampled from cyclic and acyclic aliphatic amines, benzylic amines, and amines bearing tethered aryl and heteroaryl groups. The data from this study revealed that potent PDE1B inhibition with respect to the quinazoline ring was favored with 7,8-dimethoxy functionalization, and that a third methoxy group in the 6-position was neither detrimental nor required for binding. Library-derived compounds from each of the amine classes exhibited reasonable potency (36 – 1000 nM) with the most potent analog being that derived from 6,7,8-trimethoxyquinazoline and 3-aminopentane (**7a**, PDE1B IC_{50} = 35 nM, Figure 3). The nature of the amino substituent in this series was judged to be relatively non-critical for PDE1 inhibitory potency, in contrast to the case of PDE10A which strongly prefers amine substituents with associated aryl

groups.[16]

In our second approach to SAR expansion we launched a search for quinazoline replacements that would yield additional active compounds. For example, good PDE10A potency is available from quinazoline, phthalazine, and cinnoline templates (compounds **8-10**, Figure 4a).[23] However, in the PDE1B series potent inhibition was only available from the quinazoline template (**11**), with phthalazine, cinnoline, quinoline and isoquinoline templates each affording inactive compounds (**12-15**, 0% inhibition at 1 uM, Figure 4b).

Figure 4a: PDE10A inhibitors

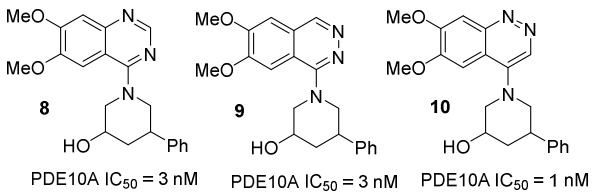

Figure 4b: PDE1B inhibition

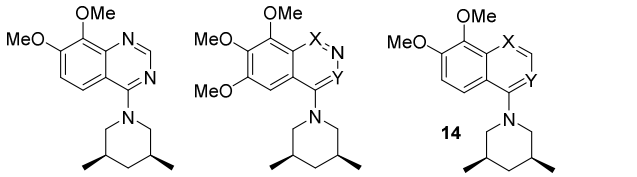

Figure 4. Quinazoline vs. cinnoline, phthalazine, quinoline and isoquinoline structures.

The X-ray crystal structure of **7a** bound to the catalytic subunit of PDE1B provided an explanation for the quinazoline structural requirement. Relative to similar PDE10A inhibitors, in PDE1B the quinazoline is rotated slightly (counter-clockwise vs. Figure 2) such that the quinazoline 7- and 8- methoxy groups accept a bifurcated H-bond from the side chain nitrogen of the PDE1 Gln-421 residue, rather than the 6- and 7-methoxy groups in PDE10A inhibitors (Figure 5). This rotation positions the key quinazoline N1 atom to accept a hydrogen bond from the imidazole side chain of His-373, which is absent in PDE10A. The requirement for a quinazoline core in this series is further explained by the hydrogen bonding pattern at quinazoline-N3, which is 2.8 Å from a crystallographic water molecule. This water molecule is in turn coordinated by hydrogen bonds to the side chain phenol of Tyr-222 (2.7 Å), to the carbonyl of Asp-370 (2.6 Å), and to the catalytic Zn atom via a second well-ordered crystallographic water molecule. This network of water-mediated hydrogen bonds is likely important for quinazoline potency. This contention is reinforced by the observation that both the cinnoline and quinoline templates, which retain N1 but lack the hydrogen bond acceptor at position 3, show no activity against PDE1B (Figure 4b). The C4-amine donates a hydrogen bond to a crystallographic water molecule but does not appear to make productive interactions with the PDE1B catalytic subunit. The 6-methoxy group likewise contributes no productive protein-ligand interactions with the subunit and is instead oriented towards solvent.

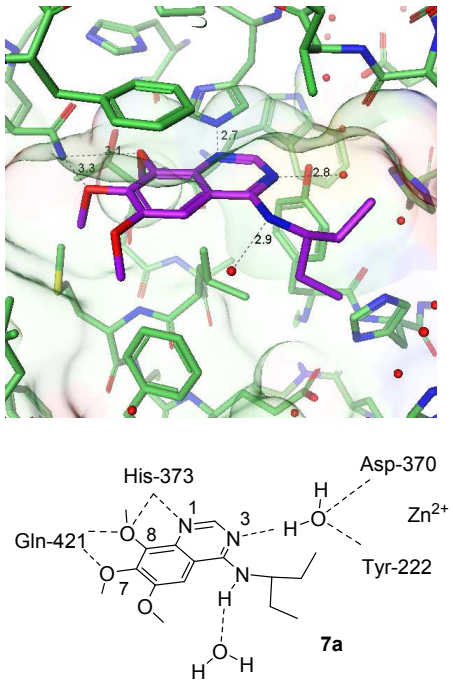

Figure 5. X-ray structure the of PDE1B/7a complex (top) and schematic representation (RCSB accession code 4NPV).

Synthesis of the 4-benzyl quinazoline series was generally accomplished by enolate addition of methyl aryl acetates (**16**) to the 4-chloroquinazolines to give the esters **17**. Subsequent saponification/decarboxylation yielded the final targets **18** as shown in Figure 6. This sequence could be conveniently accomplished in one vessel by quenching the enolate reaction mixture with aqueous sodium hydroxide to induce saponification/decarboxylation. For indanes such as **21b** and **23b** (Figure 7), better results were obtained through isolation of the ester adduct (i.e. **21a** and **23a**) prior to saponification. An oxygen-free environment was necessary during saponification of the indane derivative **23a** to minimize quinazoline decomposition via the alcohol **26**, which occurs under strongly basic conditions in air. This oxygen free environment was maintained by holding the reaction at a steady reflux during the saponification or by conducting the saponification rapidly via microwave irradiation in degassed solvent. Efforts to avoid this decomposition by employing HCl or H_2SO_4 catalyzed ester hydrolysis were not successful due to the instability of the quinazoline products to strong acid. Pure samples of the indanes **23b** and **27** were found to be stable for several months during normal bench-top storage.

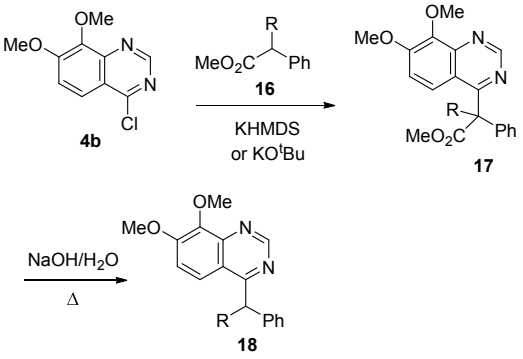

Figure 6. Synthesis of 4-benzylquinazoline derivatives.

SAR development of the benzyl series is summarized in Figure 7. Removal of the chlorine atom and the benzylic methyl group is detrimental to binding (cf. **19**, **20** and **2**), and structure rigidification yields potency improvements as evidenced by the indane derivative **21b**. As anticipated based on 4-amino-quinazoline SAR and the X-ray structure, transposition of the quinazoline 6-methoxy group to the 8-position afforded a significant potency boost (**2** vs. **22**). Replacement of the chlorine atom with bromine or fluorine yielded potency losses in the indane set (**23b** vs. **24** and **25**), possibly indicating the presence of a hydrophobic pocket appropriately sized to accommodate chlorine (see modeling discussion below).

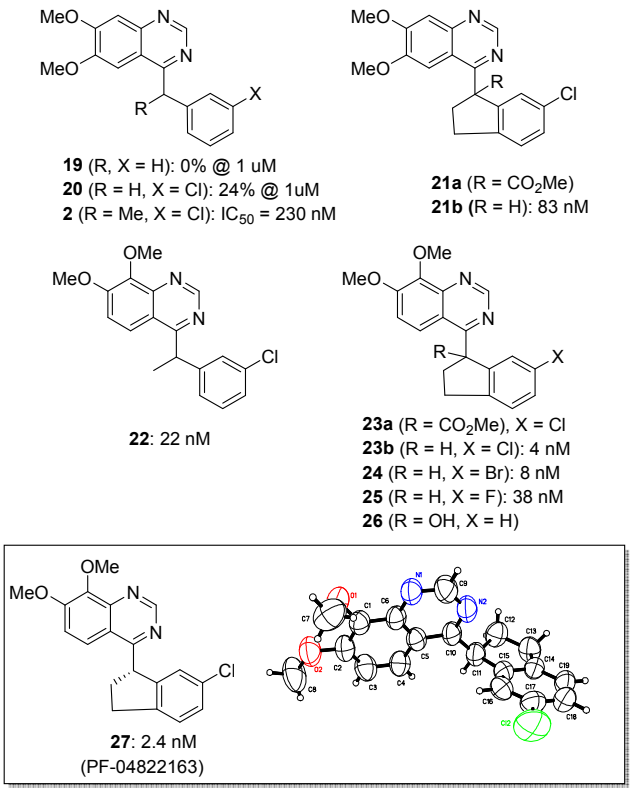

Figure 7. SAR of PDE1B inhibition by 4-benzylquinazoline inhibitors.

The synthesis of the most potent compound of this campaign, target **27** (PDE1B IC_{50} = 2.4 nM), is shown in Figure 8. Oxidation of the nitrobenzaldeyde derivative **28** to the corresponding carboxylic acid **29** and subsequent nitro group reduction afforded the anthranilic acid derivative **30**. Conversion into quinazolone **31** was followed by $POCl_3$ treatment to yield the requisite 4-chloroquinazoline **4b**. The chloroindane methyl ester **34** was prepared by direct chlorination of the indane acid **32**[24-26] and selective recrystallization of **33** (see Supporting Information) followed by esterification. Coupling with the quinazoline **4b** was accomplished via the enolate addition/decarboxylation procedure (vide supra) to give racemic **23b**, and chiral HPLC resolution afforded the final product **27**. X-ray crystallography was used to establish absolute stereochemical configuration as the (*S*) configuration as shown (see Supporting Information).

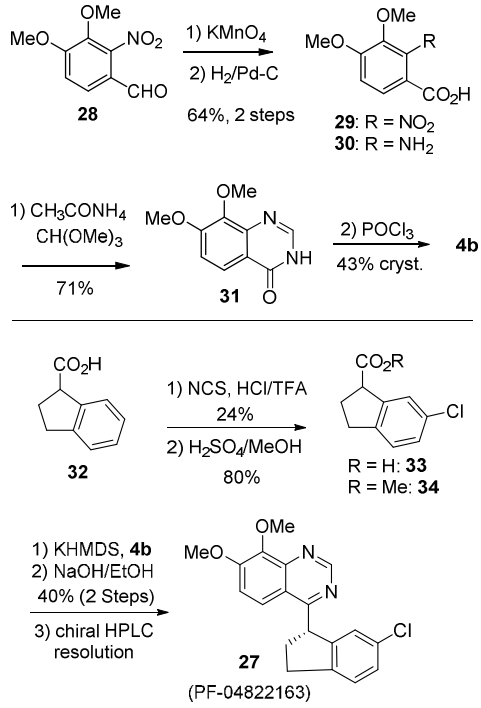

Figure 8. Synthesis of benzylquinazoline **27**.

Limited attempts to crystallize derivative **27** bound to the PDE1B catalytic subunit were not successful, but computer modeling studies summarized in Figure 9 provide a reasonable description of possible protein/ligand interactions. The quinazoline ring likely forms the same interactions as described for the X-ray structure of bound **7a**. In this orientation the chlorine atom is well positioned to occupy the hydrophobic pocket defined by Leu-388 and Phe-392. Significantly greater affinity for **27** over its enantiomer (IC_{50} = 2 nM vs. 458 nM) suggest a key role for the chiral center in projecting the chlorine atom towards this pocket.

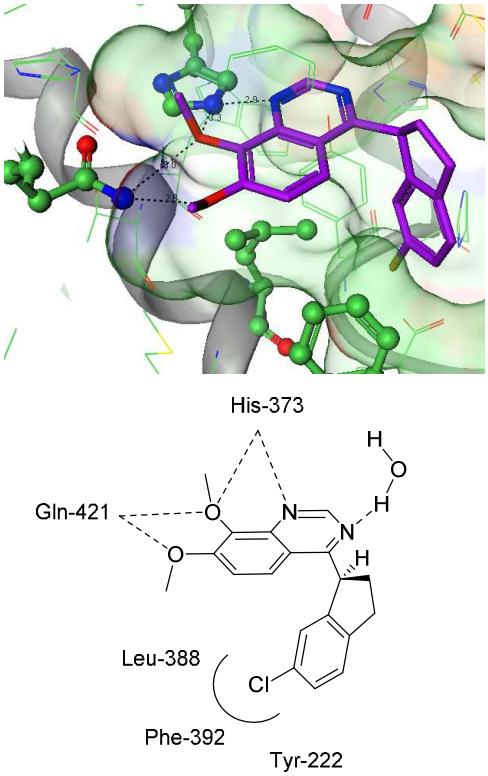

Figure 9. Computer generated model of benzylquinazoline **27** docked within the active site of PDE1B (top), and schematic representation.

The quinazoline **7a** presents a simple structure with favorable attributes for CNS penetration (MW = 305, cLogP = 4.2, TPSA = 66).[27] The compound forms a highly water soluble hydrochloride salt, has good cell permeability, and is not an efflux substrate. The potencies of **7a** for inhibition of recombinant full length and catalytic domain PDE1A, PDE1B, and PDE1C varied by less than 2-fold, which in addition to the crystal structure data suggests that **7a** is a catalytic-site competitive inhibitor. Compound **7a** exhibits > 100-fold selectivity for PDE1B and > 30-fold selectivity for PDE1A over other PDE isoforms (Table 1),[28-30] showed little activity when screened against a wide panel of biologically relevant enzymes and receptors (Supporting Information)[31] and does not inhibit the binding of dofetilide to the hERG ion channel. Compound **7a** has good stability in human liver microsomes (< 6.5 mL/min/Kg), somewhat elevated rat microsomal clearance (45 mL/min/Kg), and is rapidly absorbed into the systemic circulation after subcutaneous (sc) administration in both mouse and rat (T_{max} = 0.25 h). The sc rodent plasma half-life of **7a** is 0.25-0.66 h and it is moderately bound to plasma proteins with unbound fractions (f_u) of 10-18% (Table 3). The compound readily penetrates the blood brain barrier as indicated by brain/plasma (B/P) ratios of 0.3-0.4 that remained constant until the compound was eliminated. Concentrations of **7a** in the cerebrospinal fluid (CSF) were similar to that free in plasma (CSF/free plasma = 0.9), further indicating that the compound readily equilibrates into brain after systemic administration. When dosed orally to fed rats (50 mpk), **7a** achieved a maximal plasma concentration at 0.25 h of 3333 ng/mL (10.9 uM), and expressed a terminal half-life of 5.1 h (see additional data in Supporting Information).

Table 1. Human PDE inhibition and PDE1B selectivity for compound **7a**.

PDE	IC_{50} (nM)	Fold Selectivity
PDE1A1	118	3 x
PDE1B1	**35**	**1 x**
PDE1C1	36	1 x
PDE2A1	>30,000	>857 x
PDE3A1	>30,000	>857 x
PDE4D3	>23,600	>674 x
PDE5A1	9010	257 x
PDE6A	9260	264 x
PDE7B	>30,000	>857 x
PDE8B	>30,000	>857 x
PDE9A1	>30,000	>857 x
PDE10A1	4820	138 x
PDE11A4	3780	108 x

Compound **27** presents a more complex structure, possessing a single chiral center and requiring a more challenging synthesis. The non-basic compound does not form a hydrochloride salt, and is sparingly water soluble. Other physical properties are consistent with excellent brain penetrability (MW = 340, cLogP = 4.8, TPSA = 44). The compound is a more potent inhibitor of PDE1 than **7a** and likewise does not offer appreciative PDE1 isoform selectivity. It exhibits >105 x selectivity for PDE1B and 36 x selectivity for PDE1A over other PDE isoforms. Broad receptor and enzyme profiling (Supporting Information) reveals that the **27** interacts with serotonin and adenosine receptors (5HT2B IC_{50} = 250 nM; Adenosine A3 IC_{50} = 370 nM) and is an inhibitor of cytochrome P450 2C19 (IC_{50} = 870 nM). The compound is highly bound to plasma proteins (f_u = 2.8%) and when dosed orally at 50 mpk in the rat it achieves plasma T_{max} of 274 ng/mL (806 nM) at 0.5 h (Table 3) with a terminal half-life of 5.5 h. Plasma exposure appears to plateau between the 50 mg/Kg and 200 mg/Kg oral doses, possibly due to solubility limited absorption. While nearly 3x greater plasma exposures were achieved with sc dosing, a similar plateau event was observed between the 50 mg/Kg and 200 mg/Kg doses. (see additional data in Supporting information). The compound is readily absorbed into the CNS (B/P = 3.4) and CSF concentrations were slightly higher than that in free plasma (CSF/free plasma = 1.7), further illustrating unimpeded brain penetration.

Table 2. Human PDE inhibition and PDE1B selectivity for compound **27**.

PDE	IC_{50} (nM)	Fold Selectivity
PDE1A1	2	0.8 x
PDE1B1	**2.4**	**1 x**
PDE1C1	7	2.9 x
PDE2A1	5895	2456 x
PDE3A1	>30,000	>12,500 x
PDE4D3	7620	3175 x
PDE5A1	>30,000	>12,500 x
PDE6A	>29500	>12,292 x
PDE7B	>29800	>12,416 x
PDE8B	3467	1,444 x
PDE9A1	>30,000	>12,500 x
PDE10A1	252	105 x
PDE11A4	8257	3,440 x

Table 3. Select PK data for **7a** and **27** in rat and mouse[a]

Compd.	Species	Dose[b]	T_{max} (h)	$t_{1/2}$	f_u	B/P	CSF/P_u
7a	Mouse	32	0.25	2.0 h	0.18	0.28	--
7a	Rat	10	0.25	0.66 h	0.10	0.4	0.9
27	Rat	10	0.5	--	0.028	3.4	1.7

[a] mpk = mg/Kg; sc = subcutaneous; $t_{1/2}$ = half-life; f_u = fraction unbound; B/P = brain/plasma; P_u = unbound fraction in plasma.
[b]Doses were administered subcutaneously; units are mg/Kg.
Extensive additional data may be found in the Supporting Information.

Conclusions

In conclusion, we have disclosed a new class of selective, CNS penetrable quinazoline PDE1 inhibitors discovered through SAR development of two file screen hits. In a combination of parallel and traditional organic synthesis, and with the aid of X-ray crystallography and molecular modeling, structural refinement of the lead compounds led to the aminoquinazoline **7a** (PF-04471141) and the indanylquinazoline **27** (PF-04822163). These compounds are among the most potent and selective inhibitors of PDE1 reported to date. Pharmacokinetic investigations in rodents indicate that each compound achieves systemic concentrations in excess of their IC_{50} values. Thus, compounds **7a** and **27** offer considerable potential as chemical probes to further investigate biological processes of the CNS impacted by PDE1 function, and to assess the potential of pan-PDE1 inhibition as a therapy for the treatment of neuropsychiatric illness.

Notes and references

[a] *Neuroscience Medicinal Chemistry, Pfizer World Wide Research and Development, Eastern Point Road, Groton, CT 06340, USA. E-mail: john.m.humphrey@pfizer.com.*
[b] *Safety Pharmacology CoE, Pfizer World Wide Research and Development, 10646 Science Center Drive, San Diego, CA 92121, USA.*
[c] *Pfizer World Wide Research and Development, 620 Memorial Drive, Cambridge, MA 02139, USA.*
[d] *Pharmaceuticals, Inc. One Davol Square, Suite 105, Providence, RI 02903. E-mail: fmenniti@mnemosynepharma.com.*

† Electronic Supplementary Information (ESI) available: Broad panel ligand-receptor binding data, PDE1 assay data with standard error, select pharmacokinetic data for **7a** and **27**, X-ray crystal structure experimental information for **7a** and **27**, PDE1B1 enzyme purity data and binding assay protocol, and complete synthesis experimental details. The crystal structure of inhibitor 7a bound to the PDE10A catalytic subunit has been deposited to the RCSB protein data bank with the entry code 4NPV.

‡ Abbreviations Used: (±) denotes a racemic compound; PDE, phosphodiesterase; cAMP, cyclic adenosine monophosphate; cGMP, cyclic guanosine monophosphate; CNS, central nervous system; cryst, crystallized; LTP, long term potentiation; LTD, long term depression; NCS, N-chlorosuccinimide; PCP, phencyclidine; PK, pharmacokinetics; rt, room temperature; sc, subcutaneous; TFA, trifluoroacetic acid.

Compound **7a**, also known as PF-04471141 or its hydrochloride salt PF-04471141-01, is now commercially available from Sigma Aldrich.

.

(1) Beavo, J. A. *Physiol. Rev.* 1995, ***75***, 725.
(2) Conti, M.; Beavo, J. *Annual Review of Biochemistry* 2007, **76**, 481.
(3) Mehats, C.; Andersen, C. B.; Filopanti, M.; Jin, S. L. C.; Conti, M. *Trends Endocrinol Metab* 2002, **13**, 29.
(4) Lugnier, C. *Pharmacol. Ther.* 2006, **109**, 366.
(5) Menniti, F. S.; Faraci, W. S.; Schmidt, C. J. *Nat. Rev. Drug Discovery* 2006, ***5***, 660.
(6) Bender, A. In *Cyclic nucleotide Phosphodiesterases in Health and Disease*; Beavo, J. A. F., SH; Houslay, MD, Ed.; CRC press: 2006, p 35.
(7) Cheung, Y. *Biochemical and Biophysical Research Communications* 1970, **38**, 533.
(8) Kakiuchi, S. Y., R *Biochemical and Biophysical Research Communications* 1970, **41**, 1104.
(9) Yan, C.; Zhao, A. Z.; Bentley, J. K.; Loughney, K.; Ferguson, K.; Beavo, J. A. *Proceedings of the National Academy of Sciences of the United States of America* 1995, **92**, 9677.
(10) Yan, C.; Bentley, J.; Sonnenburg, W.; Beavo, J. *J. Neurosci.* 1994, **14**, 973.
(11) Reed, T. M.; Repaske, D. R.; Snyder, G. L.; Greengard, P.; Vorhees, C. V. *J. Neurosci.* 2002, **22**, 5188.
(12) Wong, M.-L.; Whelan, F.; Deloukas, P.; Whittaker, P.; Delgado, M.; Cantor, R. M.; McCann, S. M.; Licinio, J. *Proceedings of the National Academy of Sciences* 2006, **103**, 15124.
(13) Blokland, A.; Menniti, F. S.; Prickaerts, J. *Expert Opin. Ther. Pat.* 2012, ***22***, 349.
(14) Gupta, S.; Sharma, B. *Eur. J. Pharmacol.* 2014, **732**, 111.
(15) A series of potent PDE1 inhibitors has been described with one example achieving a PDE1 IC_{50} of 0.07 nM. While members of the series can achieve good selectivty for PDE1 over PDE5 and vice-versa, full selectivity data vs. the other PDE families (PDE2, PDE4, and PDE's 6-11) was not reported. See Ahn, H.-S. et al., J. Med. Chem. 1997, **40**, 2196-2210.
(16) Chappie, T. A.; Humphrey, J. M.; Allen, M. P.; Estep, K. G.; Fox, C. B.; Lebel, L. A.; Liras, S.; Marr, E. S.; Menniti, F. S.; Pandit, J.; Schmidt, C. J.; Tu, M.; Williams, R. D.; Yang, F. V. *J. Med. Chem.* 2007, **50**, 182.
(17) Wager, T. T.; Chandrasekaran, R. Y.; Hou, X.; Troutman, M. D.; Verhoest, P. R.; Villalobos, A.; Will, Y. *ACS Chem. Neurosci.* 2010, **1**, 420.

(18) Wager, T. T.; Hou, X.; Verhoest, P. R.; Villalobos, A. *ACS Chem. Neurosci.* 2010, **1**, 435.
(19) Takase, Y.; Watanabe, N.; Adachi, H.; Kodama, K.; Ishihara, H.; Saeki, T.; Souda, S.; WO9507267, Esai Co, L., Ed. 1995.
(20) Pamukeu, R.; Piazza, G.; US5990117, Cell Pathways, I., Ed. USA, 1999.
(21) Takase, Y.; Saeki, T.; Fujimoto, M.; Saito, I. *J. Med. Chem.* 1993, **36**, 3675.
(22) Takase, Y.; Saeki, T.; Watanabe, N.; Adachi, H.; Souda, S.; Saito, I. *J. Med. Chem.* 1994, **37**, 2106.
(23) Humphrey, J. M.; Chappie, T. A.; Liras, S.; US0019975A1, Pfizer Inc, USA . 2006, p 32 pp.
(24) Katz, C. E.; Aube, J. *J. Am. Chem. Soc.* **2003**, *125*, 13948.
(25) Mermerian, A. H.; Fu, G. C. *J. Am. Chem. Soc.* 2005, **127**, 5604.
(26) Aono, T.; Kishimoto, S.; Araki, Y.; Noguchi, S. *Chem Pharm Bull (Tokyo)* 1977, **25**, 3198.
(27) Wager, T. T.; Chandrasekaran, R. Y.; Hou, X.; Troutman, M. D.; Verhoest, P. R.; Villalobos, A.; Will, Y. *ACS Chem. Neurosci.*, *1*, 420.
(28) Siuciak, J. A.; Chapin, D. S.; Harms, J. F.; Lebel, L. A.; McCarthy, S. A.; Chambers, L.; Shrikhande, A.; Wong, S.; Menniti, F. S.; Schmidt, C. J. *Neuropharmacology* 2006, **51**, 386.
(29) Verhoest, P. R.; Chapin, D. S.; Corman, M.; Fonseca, K.; Harms, J. F.; Hou, X.; Marr, E. S.; Menniti, F. S.; Nelson, F.; O'Connor, R.; Pandit, J.; Proulx-LaFrance, C.; Schmidt, A. W.; Schmidt, C. J.; Suiciak, J. A.; Liras, S. *J. Med. Chem.* 2009, **52**, 5188.
(30) Schmidt, C. J.; Chapin, D. S.; Cianfrogna, J.; Corman, M. L.; Hajos, M.; Harms, J. F.; Hoffman, W. E.; Lebel, L. A.; McCarthy, S. A.; Nelson, F. R.; Proulx-LaFrance, C.; Majchrzak, M. J.; Ramirez, A. D.; Schmidt, K.; Seymour, P. A.; Siuciak, J. A.; Tingley, F. D., III; Williams, R. D.; Verhoest, P. R.; Menniti, F. S. *J. Pharmacol. Exp. Ther.* 2008, **325**, 681.
(31) Broad receptor profiling was accomplished by Cerep, Inc., Redmond, WA.

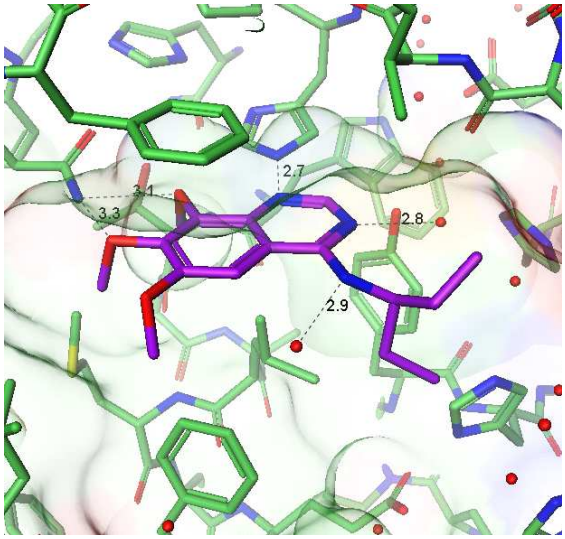

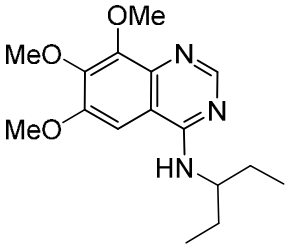

7a
(PF-04471141)
PDE1B IC_{50} = 35 nM

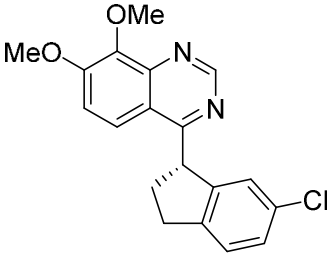

27
(PF-04822163)
PDE1B IC_{50} = 2.4 nM

ABSTRACT: PDE1 is a family of calcium-activated, dual substrate phosphodiesterases expressed in both the CNS and periphery that play a role in the integration of intracellular calcium and cyclic nucleotide signaling cascades. Exploration of the potential in targeting this family of enzymes to treat neuropsychiatric disorders has been hampered by a lack of potent, selective, and brain penetrable PDE1 inhibitors. To identify such compounds we used high-throughput screening, structure-based design, and targeted synthetic chemistry to discover the 4-aminoquinazoline **7a** (PF-04471141) and the 4-indanylquinazoline **27** (PF-04822163) each of which are PDE1 inhibitors that readily cross the blood brain barrier. These quinazoline-based PDE1-selective inhibitors represent valuable new tools to study the biological processes regulated by PDE1 and to begin to determine the potential therapeutic utility of such compounds to treat neuropsychiatric disorders.